

On the wavefront spacing of focused, radially polarized beams

Taco D. Visser

Department of Physics and Astronomy, Free University, De Boelelaan 1081, 1081 HV Amsterdam, The Netherlands

John T. Foley

Department of Physics and Astronomy, Mississippi State University, Mississippi State, Mississippi 39762

Received February 12, 2005; accepted March 28, 2005

We analyze the phase behavior of strongly focused, radially polarized electromagnetic fields. It is shown that, under certain circumstances, the spacing between successive wavefronts can be either greater or smaller than that of a plane wave of the same frequency. Also, this spacing can be significantly larger than that which is predicted for a linearly polarized field that is focused by the same system. © 2005 Optical Society of America
OCIS codes: 050.1960, 140.3300, 260.2110, 260.5430.

1. INTRODUCTION

Radially polarized beams^{1,2} have several interesting properties. For example, they exhibit an on-axis phase singularity. Also, when such a beam is focused, the field in the focal region has a strong longitudinal component with a spot size that is smaller than that of a linearly polarized beam.^{3–5} Possible applications of focused radially polarized beams are the probing of the dipole moment of individual molecules,⁶ high-resolution microscopy,⁷ and the trapping of metallic particles.⁸

It has long since been thought that the wavefront spacing of focused fields is larger than that of a plane wave of the same frequency. Linfoot and Wolf found within the scalar approximation that the wavefronts in the focal region are separated by a distance $\lambda/(1-a^2/4f^2)$, where λ denotes the wavelength, a denotes the aperture radius, and f denotes the focal length of the lens.⁹ It follows from this expression that the wavefronts are equidistant and that their spacing increases with increasing numerical aperture (NA). The aim of the present paper is to investigate the wavefront spacing for radially polarized beams that are focused by a high-NA system.

The wavefront spacing of focused, linearly polarized beams has recently been investigated by Foley and Wolf.¹⁰ They showed that, in systems of high-NA, the wavefront spacing near the focus is significantly larger than the wavelength of the incident light and that the wavefront spacing changes drastically within a few wavelengths of the focus and can be less than a wavelength.

2. RADIALLY POLARIZED BEAMS

There are several ways to generate a radially polarized beam.^{5,11} Perhaps the simplest approach is the superposition of two, mutually orthogonally polarized, Hermite–Gaussian beams.^{6,12} The time-independent part of the

electric field distribution of the TEM₁₀ and TEM₀₁ modes traveling in the positive z direction is given by the expressions¹³

$$\begin{aligned} \tilde{\mathbf{E}}_{10}(x,y,z) &= \frac{2^{3/2}Aw_0}{w^2(z)} x\hat{\mathbf{x}} \exp\{i[kz - 2 \tan^{-1}(z/z_0)]\} \\ &\quad \times \exp[ik(x^2 + y^2)/2R(z)] \exp[-(x^2 + y^2)/w^2(z)], \end{aligned} \quad (1)$$

$$\begin{aligned} \tilde{\mathbf{E}}_{01}(x,y,z) &= \frac{2^{3/2}Aw_0}{w^2(z)} y\hat{\mathbf{y}} \exp\{i[kz - 2 \tan^{-1}(z/z_0)]\} \\ &\quad \times \exp[ik(x^2 + y^2)/2R(z)] \exp[-(x^2 + y^2)/w^2(z)]. \end{aligned} \quad (2)$$

Here $k = \omega/c$ is the wavenumber, with ω and c as, respectively, the angular frequency and the speed of light in vacuum and with $\hat{\mathbf{x}}$ and $\hat{\mathbf{y}}$ as unit vectors in the x and y directions. Furthermore, A is a constant, and w_0 is the spot size of the beam in the waist plane $z=0$. The radius of curvature $R(z)$, the spot size $w(z)$, and the Rayleigh range z_0 are given by the formulas

$$R(z) = z + z_0^2/z, \quad (3)$$

$$w(z) = w_0(1 + z^2/z_0^2)^{1/2}, \quad (4)$$

$$z_0 = \pi w_0^2/\lambda. \quad (5)$$

The total electric field of the beam, $\mathbf{E}(x,y,z,t)$, is given by the equation

$$\mathbf{E}(x,y,z,t) = [\tilde{\mathbf{E}}_{10}(x,y,z) + \tilde{\mathbf{E}}_{01}(x,y,z)] \exp(-i\omega t), \quad (6)$$

where t denotes the time. On substituting from Eqs. (1) and (2) into Eq. (6), we obtain the expression

$$\mathbf{E}(\rho, z, t) = \frac{2^{3/2} A w_0}{w^2(z)} \hat{\rho} l_0(\rho) \exp\{i[kz - 2 \tan^{-1}(z/z_0)]\} \times \exp(-i\omega t), \quad (7)$$

with $\rho = (x^2 + y^2)^{1/2}$ and $\hat{\rho} = (x, y, 0)/\rho$ as a unit vector in the radial direction. The radial amplitude function $l_0(\rho)$ is given by the formula

$$l_0(\rho) = \rho \exp[ik\rho^2/2R(z)] \exp[-\rho^2/w^2(z)]. \quad (8)$$

Note that the radially polarized beam described by Eq. (7) is completely characterized by the three parameters A , λ , and w_0 .

3. FOCUSING BY SYSTEMS WITH A HIGH NUMERICAL APERTURE

When a beam of light is focused by a high-angular-aperture system, classical scalar theory no longer applies, and the vector character of the field has to be taken into account.¹⁴ Wolf and co-workers analyzed the field in the focal region of such a system for the case of a linearly polarized beam.^{15–19} The focusing of radially polarized beams has been analyzed by Youngworth and Brown.^{11,20} We follow their analysis, but we adopt the sign convention of Richards and Wolf.¹⁷

Consider an aplanatic focusing system L , as illustrated in Fig. 1. The system has a focal length f and a semiaperture angle α , and hence its $\text{NA} = \sin \alpha$. The geometrical focus is indicated by O and is chosen to be the origin of the coordinate system. A monochromatic beam is incident on the system. The electric and magnetic fields at time t at position \mathbf{r} are given by the expressions

$$\mathbf{E}(\mathbf{r}, t) = \text{Re}[\mathbf{e}(\mathbf{r}) \exp(-i\omega t)], \quad (9)$$

$$\mathbf{H}(\mathbf{r}, t) = \text{Re}[\mathbf{h}(\mathbf{r}) \exp(-i\omega t)], \quad (10)$$

respectively, where Re denotes the real part. It was shown by Richards and Wolf¹⁷ that the time-independent parts, \mathbf{e} and \mathbf{h} , of the electric and magnetic fields in the focal region can be expressed as a superposition of plane waves, i.e.,

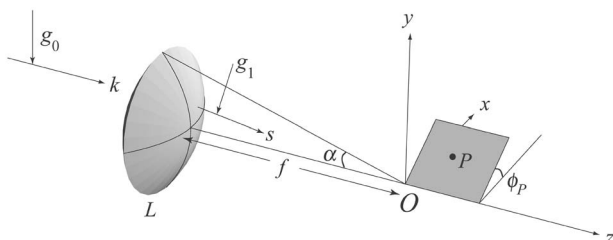


Fig. 1. Illustration of a high-NA focusing system. The incident beam propagates along the z axis.

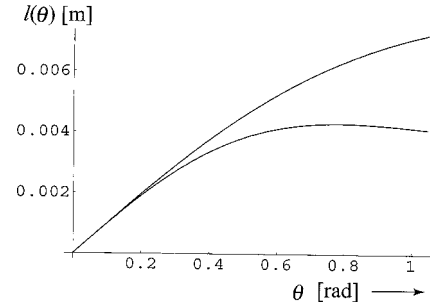


Fig. 2. Example of the angular amplitude function $l(\theta)$ for two different values of the beam-spot size w_0 . For the upper curve $w_0 = 0.02$ m, for the lower curve $w_0 = 0.01$ m. In both cases $f = 0.01$ m.

$$\mathbf{e}(\mathbf{r}) = -\frac{ik}{2\pi} \iint_{\Omega} \frac{\mathbf{a}(s_x, s_y)}{s_z} \exp[ik(s_x x + s_y y + s_z z)] ds_x ds_y, \quad (11)$$

$$\mathbf{h}(\mathbf{r}) = -\frac{ik}{2\pi} \iint_{\Omega} \frac{\mathbf{b}(s_x, s_y)}{s_z} \exp[ik(s_x x + s_y y + s_z z)] ds_x ds_y. \quad (12)$$

The unit vector $\mathbf{s} = (s_x, s_y, s_z)$ indicates the direction of propagation of each wave. The set of all vectors \mathbf{s} spans the geometrical light cone Ω . The strength factors \mathbf{a} and \mathbf{b} can be determined by a ray-tracing procedure.

It is advantageous to express the vector \mathbf{s} in spherical polar coordinates, i.e.,

$$\mathbf{s} = (\sin \theta \cos \phi, \sin \theta \sin \phi, \cos \theta). \quad (13)$$

Let us also introduce two unit vectors \mathbf{g}_0 and \mathbf{g}_1 in the meridional plane of the ray, such that \mathbf{g}_0 is perpendicular to the ray in the object space and \mathbf{g}_1 is perpendicular to the ray in the image space:

$$\mathbf{g}_0 = (-\cos \phi, -\sin \phi, 0), \quad (14)$$

$$\mathbf{g}_1 = (-\cos \theta \cos \phi, -\cos \theta \sin \phi, \sin \theta). \quad (15)$$

In the object space the inward radial direction is along \mathbf{g}_0 , and the azimuthal direction is along $\mathbf{g}_0 \times \mathbf{k}$, where \mathbf{k} is a unit vector along the z axis, the direction of propagation of the incident beam. In general, the electric field in the object space, $\mathbf{e}^{(0)}$, can be written as the sum of a radial part, $e_r^{(0)}$, and an azimuthal part, $e_\phi^{(0)}$, namely,

$$\mathbf{e}^{(0)} = l_0(\rho) [e_r^{(0)} \mathbf{g}_0 + e_\phi^{(0)} (\mathbf{g}_0 \times \mathbf{k})], \quad (16)$$

with $l_0(\rho)$ given by Eq. (8). The refractive action of the lens rotates the radial field component from a direction specified by the vector \mathbf{g}_0 into a direction specified by the vector \mathbf{g}_1 . The azimuthal field component remains unchanged, with the azimuthal direction in the image space being along $\mathbf{g}_1 \times \mathbf{s}$. The strength factor \mathbf{a} is related to the electric field in the object space through the expression

$$\mathbf{a} = f l(\theta) \cos^{1/2} \theta [e_r^{(0)} \mathbf{g}_1 + e_\phi^{(0)} (\mathbf{g}_1 \times \mathbf{s})]. \quad (17)$$

For cylindrical vector beams focused by a system that satisfies the sine condition,^{17,21} the angular amplitude function is given by the formula $l(\theta) = l_0[\sin^{-1}(\rho/f)]$, i.e.,

$$l(\theta) = f \sin \theta \exp[ikf^2 \sin^2 \theta/2R(z)] \exp[-f^2 \sin^2 \theta/w^2(z)]. \quad (18)$$

If we assume the entrance plane of the focusing system to coincide with the waist plane of the beam ($z=0$), then the expression for the angular amplitude function reduces to

$$l(\theta) = f \sin \theta \exp[-f^2 \sin^2 \theta/w_0^2], \quad (z=0), \quad (19)$$

where w_0 is the spot size of the beam in the waist plane. An example of the angular amplitude function is shown in Fig. 2.

For an observation point P in the focal region, with cylindrical coordinates (ρ_P, ϕ_P, z_P) , the inner product appearing in Eq. (11) can be seen to be

$$\mathbf{s} \cdot \mathbf{r} = \rho_P \sin \theta \cos(\phi_P - \phi) + z_P \cos \theta. \quad (20)$$

For an incident beam that is radially polarized, the factor $e_\phi^{(0)}$ in Eq. (16) equals zero. On then substituting from Eqs. (15), (17), and (20) into Eq. (11) we obtain for the electric field in the focal region the expression

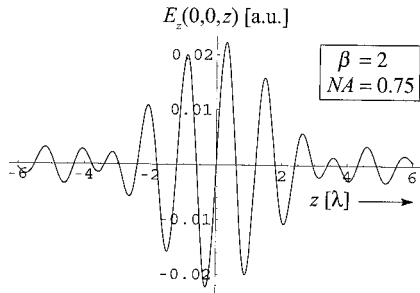


Fig. 3. Longitudinal electric field component $E_z(0,0,z)$ along the z axis. In this example, $NA=0.75$, and $\beta=f/w_0=2$.

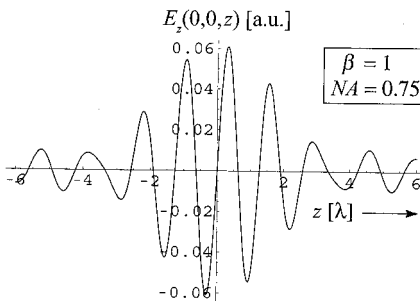


Fig. 4. Longitudinal electric field component $E_z(0,0,z)$ along the z axis. In this example, $NA=0.75$, and $\beta=f/w_0=1$.

$$\begin{aligned} \mathbf{e}(P) = & \frac{ikf}{2\pi} \int_0^\alpha \int_0^{2\pi} l(\theta) \sin \theta \cos^{1/2} \theta \\ & \times \exp\{ik[\rho_P \sin \theta \cos(\phi_P - \phi) + z_P \cos \theta]\} \\ & \times (\cos \theta \cos \phi, \cos \theta \sin \phi, -\sin \theta) d\theta d\phi, \quad (21) \end{aligned}$$

where we used the fact that $ds_x ds_y / s_z = d\Omega = \sin \theta d\theta d\phi$ and with $e_r^{(0)}$ set equal to unity.

Since the incident electric field has no azimuthal dependence and the configuration is invariant with respect to rotations around the z axis, it follows that the electric field in the focal region has no azimuthal component. The outward radial direction at a point P is specified by the vector

$$\mathbf{g}_P = (\cos \phi_P, \sin \phi_P, 0). \quad (22)$$

The electric field at P can thus be written as the sum of a radial component, $e_\rho(P)$, along \mathbf{g}_P and a longitudinal component, $e_z(P)$, along \mathbf{k} , i.e.,

$$\mathbf{e}(P) = e_\rho(P) \mathbf{g}_P + e_z(P) \mathbf{k}, \quad (23)$$

where

$$\begin{aligned} e_z(P) = & -\frac{ikf}{2\pi} \int_0^\alpha \int_0^{2\pi} l(\theta) \sin^2 \theta \cos^{1/2} \theta \\ & \times \exp\{ik[\rho_P \sin \theta \cos(\phi_P - \phi) + z_P \cos \theta]\} d\theta d\phi, \quad (24) \end{aligned}$$

$$\begin{aligned} e_\rho(P) = & \frac{ikf}{2\pi} \int_0^\alpha \int_0^{2\pi} l(\theta) \sin \theta \cos^{3/2} \theta \cos(\phi_P - \phi) \\ & \times \exp\{ik[\rho_P \sin \theta \cos(\phi_P - \phi) + z_P \cos \theta]\} d\theta d\phi. \quad (25) \end{aligned}$$

Carrying out the integration over ϕ in Eqs. (24) and (25) yields the formulas

$$\begin{aligned} e_z(P) = & -ikf \int_0^\alpha l(\theta) \sin^2 \theta \cos^{1/2} \theta \\ & \times \exp(ikz_P \cos \theta) J_0(k\rho_P \sin \theta) d\theta, \quad (26) \end{aligned}$$

Table 1. Position and Spacings (Both Expressed in Wavelengths) of the First Five Axial Zeros of the Longitudinal Electric Field Component E_z in the Focal Region of a High-NA System^a

Zero #	$\beta=2$		$\beta=1$		$\beta \rightarrow 0$	
	Position (λ)	Spacing (λ)	Position (λ)	Spacing (λ)	Position (λ)	Spacing (λ)
1	1.20	1.20	1.26	1.26	1.28	1.28
2	2.40	1.20	2.57	1.31	2.62	1.34
3	3.39	0.99	4.23	1.66	4.21	1.59
4	4.31	0.92	5.63	1.40	5.65	1.44
5	5.50	1.19	7.22	1.59	7.21	1.56

^aIn this example $NA=0.75$, and $\beta=f/w_0=2$ (column 2), $\beta=1$ (column 3), and $\beta \rightarrow 0$ (column 4).

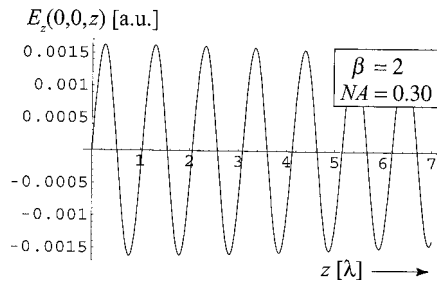


Fig. 5. Longitudinal electric field component $E_z(0,0,z)$ along the z axis. In this example $NA=0.3$, and $\beta=f/w_0=2$.

$$e_\rho(P) = -kf \int_0^\alpha l(\theta) \sin \theta \cos^{3/2} \theta \times \exp(ikz_P \cos \theta) J_1(k\rho_P \sin \theta) d\theta, \quad (27)$$

where J_i denotes the Bessel function of the first kind of order i . It is seen from Eqs. (26) and (27) that, on the z axis (i.e., $\rho_P=0$), e_z is the only nonzero part of the electric field. In Section 4 we analyze the behavior of this longitudinal field component.

4. ON-AXIS LONGITUDINAL ELECTRIC FIELD

At time $t=0$ the axial longitudinal electric field component E_z is given by the expression

$$E_z(0,0,z) = kf \int_0^\alpha l(\theta) \sin^2 \theta \cos^{1/2} \theta \sin(kz \cos \theta) d\theta, \quad (28)$$

$$= kf^2 \int_0^\alpha \sin^3 \theta \cos^{1/2} \theta \sin(kz \cos \theta) \times \exp(-\beta^2 \sin^2 \theta) d\theta, \quad (29)$$

where we used Eqs. (9), (19), and (26). The parameter $\beta \equiv f/w_0$ denotes the ratio of the focal length of the system and the spot size of the beam in the waist plane. In Figs. 3 and 4 the on-axis longitudinal electric field in the focal region of a high-NA system is shown for two selected values of the parameter β . Notice that the amplitude is strongly modulated. We define the axial intersections of the wavefronts as those points where the field $E_z(0,0,z)$ has the same phase (modulo 2π) as at the geometrical focus O . The wavefront positions and wavefront spacings corresponding to Figs. 3 and 4 are summarized in Table 1. It is seen from both examples that the spacings between the successive wavefronts are highly irregular. Notice that when $\beta=2$ the spacing can even be smaller than λ .

For the case of a spot size much larger than the focal length (i.e., $\beta \rightarrow 0$) we find a similar behavior, as is listed in the rightmost column of Table 1. [Notice that then in the waist plane of the beam the amplitude function $l_0(\rho) = \rho$, which is to be distinguished from a uniform illumination.]

It is instructive to compare our results with those of Foley and Wolf,¹⁰ who analyzed the field distribution of a focused, linearly polarized beam with a uniform amplitude.

They found the spacing between wavefronts to vary with NA value and axial position. In their examples the largest spacing always occurs next to the geometrical focus. On moving away from the focus, the spacing for high-NA systems decreases and then rises again. As can be seen from Table 1, this is not the case for radially polarized light. In particular, the largest wavefront spacing does not always occur near the focus. Another remarkable difference is that for $NA=0.75$ the maximum spacing is found to be 1.19λ for linearly polarized light, much less than the value of 1.66λ that is predicted for radially polarized light.

Our findings for high-NA systems are in stark contrast with the predictions of scalar theory, according to which the distance between successive wavefronts is constant and always greater than λ .⁹ It should be noted that the amplitude modulation and the irregular spacing of the wavefronts is found only for systems with a high-NA value. This is illustrated in Fig. 5 from which it can be seen that for $NA=0.3$ the amplitude modulation is negligible and the wavefronts are equidistant, their separation distance being 1.030λ . This value is in good agreement with scalar theory according to which the distance between successive wavefronts is 1.025λ .⁹

5. CONCLUSIONS

We have examined the wavefront spacing of the longitudinal electric field of a strongly focused, radially polarized beam. It was found that the distance between successive wavefronts is highly irregular and may be either greater or smaller than that of a plane wave of the same frequency. Also, this distance can be much larger than that which occurs for a linearly polarized beam focused by the same system. Our results have implications for the design of focusing systems with a high numerical aperture.

ACKNOWLEDGMENT

The authors thank Emil Wolf for stimulating discussions. T. D. Visser's e-mail address is tvisser@nat.vu.nl.

REFERENCES

1. R. H. Jordan and D. G. Hall, "Free-space azimuthal paraxial wave equation: the azimuthal Bessel-Gauss beam solution," *Opt. Lett.* **19**, 427-429 (1994).
2. D. G. Hall, "Vector-beam solutions of Maxwell's wave equation," *Opt. Lett.* **21**, 9-11 (1996).
3. S. Quabis, R. Dorn, M. Eberler, O. Glöckl, and G. Leuchs, "Focusing light to a tighter spot," *Opt. Commun.* **179**, 1-7 (2000).
4. S. Quabis, R. Dorn, M. Eberler, O. Glöckl, and G. Leuchs, "The focus of light—theoretical calculation and

- experimental tomographic reconstruction," *Appl. Phys. B* **72**, 109–113 (2001).
5. R. Dorn, S. Quabis, and G. Leuchs, "Sharper focus for a radially polarized light beam," *Phys. Rev. Lett.* **91**, 233901 (2003).
 6. L. Novotny, M. R. Beversluis, K. S. Youngworth, and T. G. Brown, "Longitudinal field modes probed by single molecules," *Phys. Rev. Lett.* **86**, 5251–5254 (2001).
 7. C. J. R. Sheppard and A. Choudhury, "Annular pupils, radial polarization, and superresolution," *Appl. Opt.* **43**, 4322–4327 (2004).
 8. Q. Zhan, "Trapping metallic Rayleigh particles with radial polarization," *Opt. Express* **12**, 3377–3382 (2004). <http://www.opticsexpress.org>.
 9. E. H. Linfoot and E. Wolf, "Phase distribution near focus in an aberration-free diffraction image," *Proc. Phys. Soc. London, Sect. B*, **69**, 823–832 (1956).
 10. J. T. Foley and E. Wolf, "Wave-front spacing in the focal region of high-numerical-aperture systems," *Opt. Lett.* **30**, 1312–1314 (2005).
 11. K. S. Youngworth and T. G. Brown, "Inhomogeneous polarization in scanning optical microscopy," in *Proc. SPIE* **3919**, 75–85 (2000).
 12. R. Oron, S. Blit, N. Davidson, A. A. Friesem, Z. Bomzon, and E. Hasman, "The formation of laser beams with pure azimuthal or radial polarization," *Appl. Phys. Lett.* **77**, 3322–3324 (2000).
 13. P. W. Milonni and J. H. Eberly, *Lasers* (Wiley, 1988). See especially Section 14.8.
 14. J. J. Stamnes, *Waves in Focal Region* (Hilger, 1986). See especially Chap. 16.
 15. B. Richards and E. Wolf, "The Airy pattern in systems of high angular aperture," *Proc. Phys. Soc. London, Sect. B* **69**, 854–856 (1956).
 16. E. Wolf, "Electromagnetic diffraction in optical systems I. An integral representation of the image field," *Proc. R. Soc. London, Ser. A* **253**, 349–357 (1959).
 17. B. Richards and E. Wolf, "Electromagnetic diffraction in optical systems II. Structure of the image field in an aplanatic system," *Proc. R. Soc. London, Ser. A* **253**, 358–379 (1959).
 18. A. Boivin and E. Wolf, "Electromagnetic field in the neighborhood of the focus of a coherent beam," *Phys. Rev.* **138**, B1561–B1565 (1965).
 19. A. Boivin, J. Dow, and E. Wolf, "Energy flow in the neighborhood of the focus of a coherent beam," *J. Opt. Soc. Am.* **57**, 1171–1175 (1967).
 20. K. S. Youngworth and T. G. Brown, "Focusing of high numerical aperture cylindrical-vector beams," *Opt. Express* **7**, 77–87 (2000). <http://www.opticsexpress.org>.
 21. M. Born and E. Wolf, *Principles of Optics: Electromagnetic Theory of Propagation, Interference and Diffraction of Light*, 7th (expanded) ed. (Cambridge U. Press, Cambridge, UK, 1999). See especially Sec. 4.5.1.